EPJ Web of Conferences **274**, 05010 (2022) https://doi.org/10.1051/epjconf/202227405010
*XV$^{th}$ Quark Confinement and the Hadron Spectrum*

# Aspects of chiral transition in a Hadron Resonance Gas model

*Deeptak* Biswas[1,*], *Peter* Petrezcky[2,**], and *Sayantan* Sharma[1,***]

[1]The Institute of Mathematical Sciences, a CI of Homi Bhabha National Institute, Chennai, 600113, India
[2]Physics Department, Brookhaven National Laboratory, Upton NY 11973, USA

**Abstract.** We study the chiral condensate for 2 + 1 flavor QCD with physical quarks within a non-interacting Hadron Resonance Gas (HRG) model. By including the latest information on the mass variation of the hadrons concerning the light quark mass, from lattice QCD and chiral perturbation theory, we show that it is possible to quite accurately account for the chiral crossover transition even within a conventional HRG model. We have calculated a pseudo-critical temperature $T_c$=161.2±1.6 MeV and the curvature of crossover curve $\kappa_2$=0.0203(7). These are in very good agreement with the latest continuum extrapolated results obtained from lattice QCD studies. We also discuss the limitations of extending such calculations toward the chiral limit. Furthermore, we study the effects of non-resonant hadron interactions within the HRG model and its consequences for the chiral transition in the regime of dense baryonic matter where lattice QCD results are not currently available.

## 1 Introduction

At high temperatures and(or) density the QCD matter has the chiral symmetry, which is spontaneously broken in the low-temperature hadronic phase. The breaking of the symmetry is signaled by the non-zero value of the quark (chiral) condensate, $\langle\bar{\psi}\psi\rangle \neq 0$. Lattice QCD (LQCD) estimates the symmetry restoration to happen at $T_c$ = 156.5±1.5 MeV via an analytic cross-over [1]. The hadronic phase can be described with the hadron resonance gas (HRG) model, where the attractive interactions between hadrons can be approximated by the creation of additional hadronic resonances [2, 3]. This phenomenological model is quite successful in describing the thermodynamical nature of the yield data of Heavy-Ion collisions [4, 5].

The comparison of thermodynamical observables between HRG and LQCD, establishes the validity of HRG as an effective description of the hadronic medium [6–8]. Recently strangeness related observables have demonstrated the need for additional resonances which are quark matter predicted but not listed in the Particle Data Group(PDG) [8, 9]. Although the repulsive interactions are not included in-built in the ideal HRG model, which can be included via phenomenological approaches and improves the agreement between the lattice results and HRG model [10, 11].

*e-mail: deeptakb@imsc.res.in
**e-mail: petreczk@bnl.gov
***e-mail: sayantans@imsc.res.in

In this work, we have revisited the temperature dependence of the chiral condensate in the HRG model, which was earlier addressed in [12]. With improved extraction of the quark mass derivative of the hadrons, we have extracted a very precise estimation of $T_c$ from the HRG model. We have further extended our prescription for the chiral limit and investigated the behavior of the condensate in the massless limit. We have also examined the chiral behavior at the large baryon density, with the mean-field level repulsive interaction among all the (anti-) baryons.

## 2 Chiral Condensate in the Hadron Resonance Gas model

### 2.1 Renormalized definitions of chiral condensate

The light quark condensate at non-zero temperature can be evaluated from the light quark mass derivative of the HRG pressure,

$$\langle\bar{\psi}\psi\rangle_{l,T} = \langle\bar{\psi}\psi\rangle_{l,0} + \frac{\partial P}{\partial m_l} \,, \tag{1}$$

$m_l$ is the light quark mass. We have worked with two degenerate light quarks, $m_u = m_d = m_l$. $\langle\bar{\psi}\psi\rangle_{l,0}$ is the zero temperature light quark condensate and contains multiplicative as well as additive divergences. We have used a finite observable, defined by multiplying with the strange quark mass $m_s$ [13],

$$-m_s\left[\langle\bar{\psi}\psi\rangle_{l,T} - \langle\bar{\psi}\psi\rangle_{l,0}\right] = -m_s\frac{\partial P}{\partial m_l} \,, \tag{2}$$

HotQCD Collaboration has used a dimensionless chiral condensate for non-zero quark mass [14],

$$\Delta^l_R = d + m_s r_1^4\left[\langle\bar{\psi}\psi\rangle_{l,T} - \langle\bar{\psi}\psi\rangle_{l,0}\right] \,, \tag{3}$$

here, $d = r_1^4 m_s(\lim_{m_l\to 0}\langle\bar{\psi}\psi\rangle_{l,0})^R$ and the parameter $r_1$ is derived from the static quark potential [15]. In this definition, the light quark condensate has only a multiplicative renormalization in the chiral limit. $(\lim_{m_l\to 0}\langle\bar{\psi}\psi\rangle_{l,0})^R = 2\Sigma$ and using the $SU(2)$ low energy constant of $\chi_{PT}$, $\Sigma^{1/3} = 272(5)$ MeV and $m_s = 92.2(1.0)$ MeV [16], and $r_1 = 0.3106$ fm [17], we find $d = 0.022791$.

### 2.2 Repulsive mean-field interaction

At large baryon density, the repulsive interaction among baryons starts to dominate. There are phenomenological models like excluded volume HRG model to replicate this repulsive interaction. Although the mean-field repulsion interaction provides the most sophisticated and successful formalism in explaining various susceptibilities, evaluated by Lattice QCD [11]. In the mean-field model, the pressure for the interacting ensemble of (anti-)baryons can be modeled as,

$$P_{int} = T(n_b + n_{\bar{b}}) + \frac{K}{2}(n_b^2 + n_{\bar{b}}^2) \tag{4}$$

Here the density can be written as,

$$n_b = \sum_{i=B}\int g_i\frac{d^3p}{(2\pi)^3}e^{-\beta(E_i-\mu_B+Kn_b)} \quad \text{and} \quad n_{\bar{b}} = \sum_{i=\bar{B}}\int g_i\frac{d^3p}{(2\pi)^3}e^{-\beta(E_i+\mu_B+Kn_{\bar{b}})} \tag{5}$$

The pressure from the rest of the hadrons remains the same as the ideal one. The total pressure of the HRG is then the sum of the ideal and interacting parts. The mean-field coefficient $K$ was 450 MeV fm$^3$ = 56.25GeV$^{-2}$ in Ref.[11]. In this work, we have used an extended HRG model, consisting of both the Particle Data Group mentioned and Quark Model predicted states. This list successfully describes the chiral observables and suitably estimates the pseudo-critical temperature and curvature coefficients [13]. The mean-field parameter has been modified considering this extended HRG (QMHRG). With the above prescription, one can evaluate various chiral observables from the pressure derivative, whereas the ideal HRG results can be retrieved by setting the limit $K = 0$.

### 2.3 Mass derivative of hadrons

The most important ingredient in Eq.[1] is the quark mass derivative of the hadrons i.e $\partial M/\partial m_l$. In Ref.[13], we have separately categorized all the hadrons and the resonances into different groups with different sigma terms.

The contribution of hadrons to $m_s(\partial P/\partial m_l)$ can be written as

$$m_s \frac{\partial P}{\partial m_l} = -\frac{m_s}{m_l} \sum_{\alpha} \frac{g_\alpha}{2\pi^2} \int_0^\infty dp\ p^2\ n_\alpha(E_\alpha) \frac{M_\alpha}{E_\alpha} \sigma_\alpha, \tag{6}$$

with $n_\alpha$ is the Bose-Einstein and Fermi-Dirac distribution for $\alpha \equiv$ mesons and $\alpha \equiv$ baryons respectively. The $\sigma$ terma are defined as [13],

$$\sigma_\alpha = m_l \frac{\partial M_\alpha}{\partial m_l}|_{m_l=m_l^{phys}} = m_l \langle \alpha | \bar{u}u + \bar{d}d | \alpha \rangle = M_\pi^2 \frac{\partial M_\alpha}{\partial M_\pi^2}|_{M_\pi = M_\pi^{phys}}. \tag{7}$$

The dependence of the pion and kaon masses on light and strange quark masses $m_l, m_s$ described in terms of $SU(2)$ low energy constants $F, B, \bar{l}_3, F_\pi$, are discussed in detail in Ref.[13]. Recent LQCD estimation shows $m_l \partial M_\pi/\partial m_l = M_\pi/2$ as a very good approximation [18], which is equivalent to the assumption of $M_\pi^2 = 2Bm_l$. The error on the $m_l$ derivative of $M_\pi, M_K$ can be estimated by error propagation from $B$ and $m_l$.

We have included the $\sigma$ terms for vector and iso-scalar meson ground state and categorized the rest of the meson resonances in three categories, iso-vector (like $\pi, \rho$), iso-scalar (like $\phi, \omega$), open strange ($K, K^*$ and their resonances). Ref. [19] has provided a precise determination of the $\sigma$-terms for ground state baryons. The excited states of baryon resonances have been included with the corresponding ground state $\sigma$ terms as prescribed in Ref.[13].

### 2.4 The condensate in the chiral limit

In the chiral limit of $m_l = 0$, the crossover becomes a real phase transition (second order for $\mu_B = 0$). The HRG model can not contain the information of this real transition, cause $\langle \bar{\psi}\psi \rangle_T$ will not be zero at the critical temperature $T_c^0$ as the thermal widths of the pseudo-Goldstone partners $\pi, f_0$ are not included in this model.

The pion and kaon mass squared for $m_l \to 0$ case read:

$$\frac{\partial M_\pi^2}{\partial m_l} = 2B\ ,\ \frac{\partial M_K^2}{\partial m_l} = 2B\ B_K(m_s) m_s \frac{\lambda_1(m_s) + \lambda_2(m_s)}{F^2}\ . \tag{8}$$

$B = \Sigma/F^2 = 2.76$ GeV, [16]. Pions, being the Goldstone modes of 2-flavor QCD are massless. Kaon and $\eta$ masses reduce slightly as their masses are determined primarily by the strange

quark mass. We have calculated the chiral condensate in Eq. [1] in the limit $m_l \to 0$ and normalize by its zero temperature value.

For the remaining hadrons and resonances, Eq. [2] has been rearranged in the chiral limit as

$$\lim_{m_l\to 0} \sum_\alpha \frac{\partial P_\alpha}{\partial m_l} = \lim_{m_l\to 0} \sum_\alpha \frac{\partial P_\alpha}{\partial M_\alpha}\frac{\partial M_\alpha}{\partial M_\pi^2}\frac{\partial M_\pi^2}{\partial m_l} = \frac{2B}{M^2_{\pi_{\rm phys}}} \sum_\alpha \frac{\partial P_\alpha}{\partial M_\alpha}\,\sigma_\alpha\,. \tag{9}$$

Here we have used the definition of the $\sigma$-term from Eq. [7] and normalized the right-hand side of Eq. [9] by $M^2_{\pi_{\rm phys}}$. $\lim_{m_l\to 0} \partial M_\pi^2/\partial m_l = 2B$ and the sum in Eq. [9] is over all the hadron species except for the pions and kaons. The mass modifications of the ground state baryon octet and decuplet in the chiral limit are taken following Ref. [19]. $M_\rho = 690(18)$ MeV in the chiral limit, as extracted in [13]. The uncertainty due to the chiral limit mass variation of higher mass hadrons has a negligible $\sim 1\%$ effect on $T_c$.

## 3 Results

We shall first present the results from the ideal HRG, evaluated for $\mu_B \sim 0$. Findings from the repulsive mean-field interaction will be discussed at the end of this section.

### 3.0.1 Comparison of ideal-HRG model estimations with lattice QCD

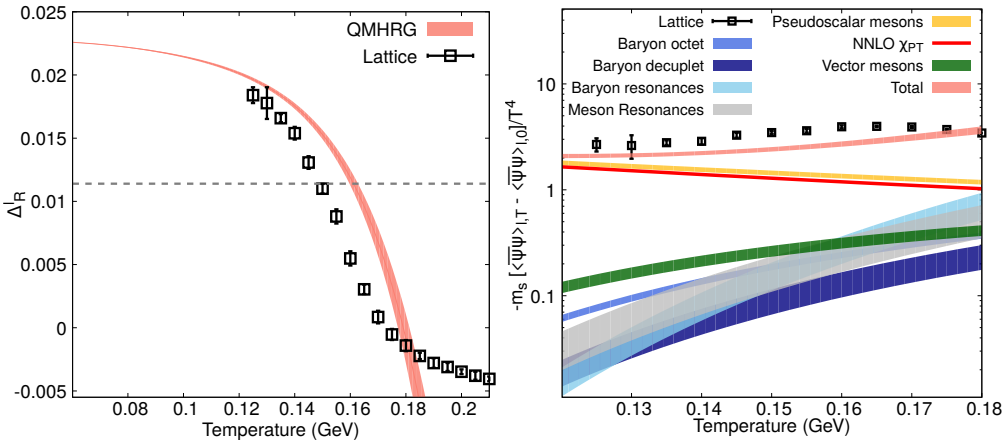


**Figure 1.** (Left) $\Delta^l_R$ is compared to the lattice data taken from Ref. [7]. The dotted line denotes the half-value of $\Delta^l_R$ compared to its magnitude at the lowest temperatures, which is used as a criterion to determine $T_c$. (Right) The relative contribution to the subtracted light quark condensate, $-m_s\left[\langle\bar\psi\psi\rangle_{l,T} - \langle\bar\psi\psi\rangle_{l,0}\right]/T^4$ due to different meson and baryon channels is shown and the resultant total contribution within QMHRG (orange band) is compared to the lattice data from Ref. [7].

The left panel of Fig. [1] shows the temperature dependence of $\Delta^l_R$ as calculated from Eq.(3) and compares with the lattice data. The difference between our HRG estimation and the LQCD results is smaller at $T \leq 140$ MeV, while for 140 MeV $< T <$ 160 MeV, the HRG model results for $\Delta^l_R$ drop slower than the lattice QCD results. The flattening of $\Delta^l_R$ in LQCD estimation signals a change in the degrees of freedom and presence of a critical temperature. The value of $T_{pc}$ depends on the observable and the corresponding normalization [20]. As the pressure in HRG increases monotonically with $T$, the renormalized chiral susceptibility

does not have an inflection point within the HRG model. Ref.[14, 21] determines $T_{pc}$ as the point where $\Delta_l^R$ drops to half of its low-temperature value. Within this definition, our ideal HRG model has estimated $T_{pc} = 161.2 \pm 1.7$ MeV.

In the right panel of Fig. [1], we have plotted the renormalized chiral condensate $-m_s\left[\langle\bar{\psi}\psi\rangle_{l,T} - \langle\bar{\psi}\psi\rangle_{l,0}\right]/T^4$ to quantify the relative contribution of different hadron species in the chiral condensate. The heavier hadrons become important for $T > 150$ MeV, and the contribution from the pseudoscalar states monotonically decreases beyond $T \sim 100$ MeV. For $T > 150$ MeV, the baryon and meson resonances start to dominate and become comparable in magnitude to the corresponding ground state. In Ref.[13] the error in $\sigma$ term for meson resonances like $\rho, K^*, \omega, \phi, \eta, \eta'$ has been improved substantially. The error bars in Fig. [1] are significant as we have assumed a 50% relative error for the $\sigma$ terms of the higher-lying meson and baryon resonances.

### 3.0.2 Curvature of the chiral crossover line from ideal HRG model

It would be interesting to investigate the crossover transition line within this prescription of HRG and $T_c$, determined with the $\Delta_R^l$. At moderately large values of $\mu_B$ the pseudo-critical temperature can be written as:

$$\frac{T_c(\mu_B)}{T_c(0)} = 1 - \kappa_2\left(\frac{\mu_B}{T_c(0)}\right)^2 - \kappa_4\left(\frac{\mu_B}{T_c(0)}\right)^4 + O(\mu_B^6)\,. \tag{10}$$

We have found that at $\mu_B = 0$, the transition temperature $T_c(0) = 161.2 \pm 1.7$ MeV. To extract the curvature terms $\kappa_2$ and $\kappa_4$, we have evaluated the pseudo-critical temperature as a function of $\mu_B$ and fitted with the Ansatz in Eq. [10] for $\mu_B/T < 1$. Our analysis results $\kappa_2 = 0.0203 \pm 0.0007$, which is in good agreement with $\kappa_2 = 0.0150(35)$, extracted from the continuum extrapolated (subtracted) chiral condensate calculated in lattice QCD [22]. However, our extracted value of $\kappa_4 = -3(2) \times 10^{-4}$ is again quite noisy, consistent with the findings from lattice QCD [1, 23]. At small baryon densities, the curvature of the pseudo-critical line is determined by $\kappa_2$ primarily, which makes the extraction of $\kappa_4$ difficult. We summarize our main findings on the curvature coefficients in the left panel of Fig. [2]. It would be interesting to extend this formalism towards large baryon density with the repulsive interaction included in the mean-field level in our forthcoming publication [24].

### 3.0.3 Chiral condensate in the massless limit

The chiral transition for two massless flavors (chiral limit) becomes a second order transition [26–28]. Recent lattice QCD estimation gives a $T_c^0 = 132^{+3}_{-6}$ MeV [29]. Even though pions will contribute dominantly to the condensate in the chiral limit, extracting the $T_c^0$ is not possible within the conventional QMHRG models which do not have the information regarding the $f_0(500)$ spectral function to accurately account for the temperature dependence of the scalar susceptibility near the transition [30].

The three-loop $\chi_{PT}$ at finite temperature, gave a $T_c^0 \sim 190$ MeV from the condition $\langle\bar{\psi}\psi\rangle_T = 0$ [25], which further reduces to $\sim 170$ MeV with the inclusion of other heavier hadrons. Right of Fig. [2] shows the ratio of chiral condensate $\langle\bar{\psi}\psi\rangle_T/\langle\bar{\psi}\psi\rangle_0$, calculated within our QMHRG list and three loop $\chi_{PT}$. This finds a transition temperature of 162. Within the QMHRG model in the chiral limit, with the ideal pion gas, a comparatively higher transition temperature $\sim 168$ MeV has been observed.

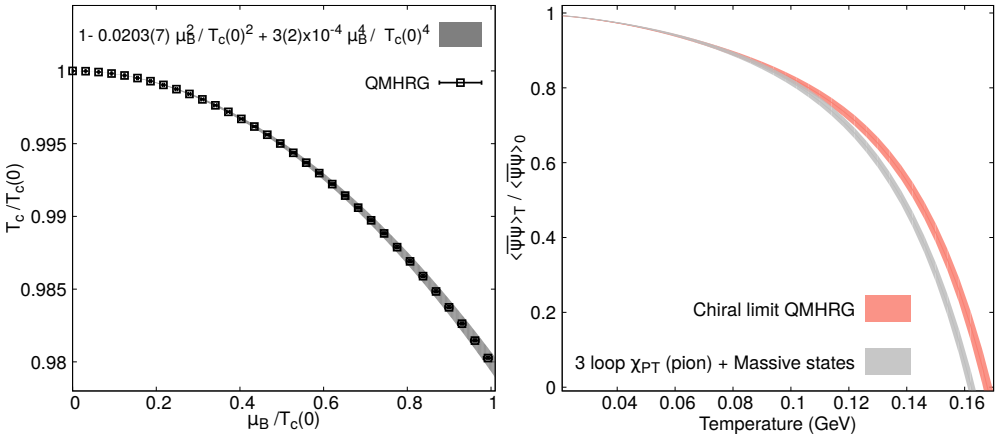


**Figure 2.** (Left) A fit to the pseudo-critical line between $\mu_B/T \lesssim 1$ gave $\kappa_2 = 0.0203(7)$ and $\kappa_4 = -3(2) \times 10^{-4}$. (Right) The ratio of the chiral condensate at a finite temperature to its zero temperature value compared to our calculation within QMHRG (orange band) compared to three loop $\chi_{PT}$ results in Ref. [25] at finite temperature $O(T^6)$ augmented by heavier hadrons used in our work (gray band).

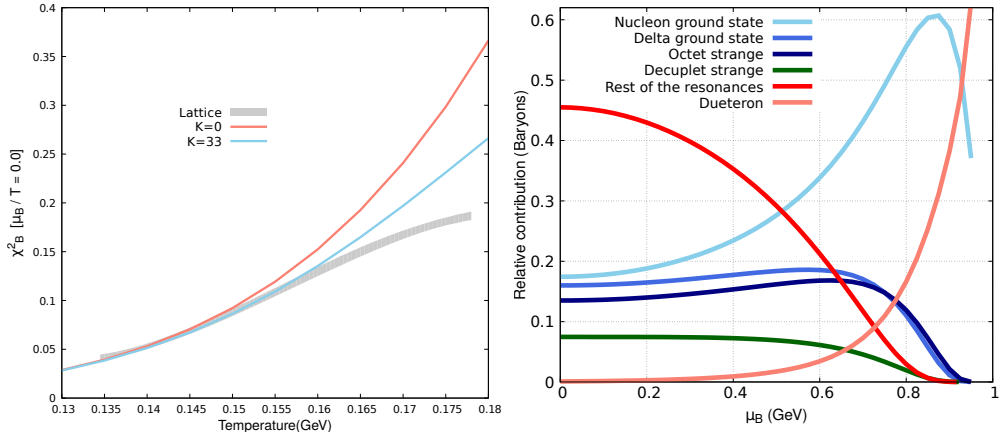


**Figure 3.** (Left) The second-order baryon number fluctuations compared between mean-field and 2 + 1 flavor QCD with physical quark masses obtained from the lattice. (Right) Variation of the relative abundance of baryons along the phase line. $x$ axis denotes the $\mu_B$, calculations are performed with the corresponding $T_c$.

### *3.0.4 HRG with Mean-field repulsion at high $\mu_B$*

At high $\mu_B$, the abundance of baryons increases, which demands the incorporation of the repulsive interaction among baryons. We have included this non-resonant interaction in the mean-field model. We estimate the mean-field parameter $K$ by comparing it with the latest lattice QCD data. For the second-order baryon number susceptibilities, the continuum extrapolated data are available as a function of temperature at $\mu_B = 0$, which allows for a reliable benchmark for comparison of the HRG model calculations and obtaining an updated value of

$K = 33$ GeV$^{-2}$. We have shown our findings with both the interacting and ideal HRG model in the left panel of Fig.[3].

In the right panel, we have shown the relative abundances of various baryons and resonances along the phase boundary calculated with the interacting HRG model [11, 24]. The nucleons start to dominate as the baryon chemical potential increases till $\mu_B \sim 0.8$ GeV. $T_c$ decreases as $\mu_B$ increases, so the thermal abundance of other heavier baryons and resonances decrease due to their higher masses. We have included the deuteron to mimic the attractive interaction between nucleons. The deuteron starts to dominate at very high baryon density due to the Boltzman factor $e^{2\mu_B/T}$. These results suggest that one should consider both the mean-field repulsive interaction and attraction among nucleons to evaluate the chiral observables and other thermodynamic observables at very high baryon density, which will be relevant in the context of Neutron stars also.

## 4 Summary and outlook

In this work, we have addressed the chiral transition for the confined state of the QCD matter. Firstly, we have used an ideal Hadron Resonance Gas formalism to investigate the chiral observables. With a precise determination of the mass derivatives of hadrons ($\sigma$ terms), we have estimated a pseudocritical temperature $T_c$=161.2±1.6 MeV. This work has also facilitated the determination of a curvature co- efficient of crossover curve $\kappa_2$=0.0203(7). These results are in good agreement with presently available results from the LQCD. We have further introduced a repulsive interaction in the mean-field level among all the baryons, which will be necessary to extend the study at the finite baryon density region.

## Acknowledgements

P.P. is supported by the U.S. Department of Energy, Office of Science, through Contract No. DE-SC0012704. S.S. gratefully acknowledges support from the Department of Science and Technology, Government of India through a Ramanujan Fellowship. D.B. acknowledges the support from IMSc and ConfXV organizers.

## References

[1] A. Bazavov et al. (HotQCD), Phys. Lett. B **795**, 15 (2019), 1812.08235
[2] R. Dashen, S.K. Ma, H.J. Bernstein, Phys. Rev. **187**, 345 (1969)
[3] R. Venugopalan, M. Prakash, Nucl. Phys. A **546**, 718 (1992)
[4] D. Biswas, Adv. High Energy Phys. **2021**, 6611394 (2021), 2003.10425
[5] D. Biswas, Phys. Rev. C **102**, 054902 (2020), 2007.07680
[6] F. Karsch, K. Redlich, A. Tawfik, Eur. Phys. J. C **29**, 549 (2003), hep-ph/0303108
[7] S. Borsanyi, Z. Fodor, C. Hoelbling, S.D. Katz, S. Krieg, C. Ratti, K.K. Szabo (Wuppertal-Budapest), JHEP **09**, 073 (2010), 1005.3508
[8] D. Bollweg, J. Goswami, O. Kaczmarek, F. Karsch, S. Mukherjee, P. Petreczky, C. Schmidt, P. Scior (HotQCD), Phys. Rev. D **104**, 074512 (2021), 2107.10011
[9] A. Bazavov et al., Phys. Rev. Lett. **113**, 072001 (2014), 1404.6511
[10] V. Vovchenko, M.I. Gorenstein, H. Stoecker, Phys. Rev. Lett. **118**, 182301 (2017), 1609.03975
[11] P. Huovinen, P. Petreczky, Phys. Lett. B **777**, 125 (2018), 1708.00879
[12] J. Jankowski, D. Blaschke, M. Spalinski, Phys. Rev. D **87**, 105018 (2013), 1212.5521

[13] D. Biswas, P. Petreczky, S. Sharma, Phys. Rev. C **106**, 045203 (2022), 2206.04579
[14] A. Bazavov et al., Phys. Rev. D **85**, 054503 (2012), 1111.1710
[15] C. Aubin, C. Bernard, C. DeTar, J. Osborn, S. Gottlieb, E.B. Gregory, D. Toussaint, U.M. Heller, J.E. Hetrick, R. Sugar, Phys. Rev. D **70**, 094505 (2004), hep-lat/0402030
[16] Y. Aoki et al. (2021), 2111.09849
[17] A. Bazavov et al. (MILC), PoS **LATTICE2010**, 074 (2010), 1012.0868
[18] G.S. Bali, S. Collins, D. Richtmann, A. Schäfer, W. Söldner, A. Sternbeck (RQCD), Phys. Rev. D **93**, 094504 (2016), 1603.00827
[19] P.M. Copeland, C.R. Ji, W. Melnitchouk (2021), 2112.03198
[20] A. Lahiri, PoS **LATTICE2021**, 003 (2022), 2112.08164
[21] A. Bazavov, P. Petreczky, Phys. Rev. D **87**, 094505 (2013), 1301.3943
[22] P. Steinbrecher, Ph.D. thesis, U. Bielefeld (main) (2018)
[23] S. Borsanyi, Z. Fodor, J.N. Guenther, R. Kara, S.D. Katz, P. Parotto, A. Pasztor, C. Ratti, K.K. Szabo, Phys. Rev. Lett. **125**, 052001 (2020), 2002.02821
[24] D. Biswas, P. Petreczky, S. Sharma (????), in preparation
[25] P. Gerber, H. Leutwyler, Nuclear Physics B **321**, 387 (1989)
[26] R.D. Pisarski, F. Wilczek, Phys. Rev. D **29**, 338 (1984)
[27] A. Butti, A. Pelissetto, E. Vicari, JHEP **08**, 029 (2003), hep-ph/0307036
[28] S. Sharma (HotQCD), *The fate of $U_A(1)$ and topological features of QCD at finite temperature*, in *11th International Workshop on Critical Point and Onset of Deconfinement* (2018), 1801.08500
[29] H.T. Ding et al. (HotQCD), Phys. Rev. Lett. **123**, 062002 (2019), 1903.04801
[30] S. Ferreres-Solé, A. Gómez Nicola, A. Vioque-Rodríguez, Phys. Rev. D **99**, 036018 (2019), 1811.07304